

Spatial and Temporal Control of Nucleation by Localized DC Electric Field

Zoubida Hammadi, Jean-Pierre Astier, Roger Morin, and Stéphane Veesler*

Centre Interdisciplinaire de Nanosciences de Marseille, CNRS, Aix-Marseille Université, CINAM-UPR3118, Campus de Luminy, Case 913, 13288 Marseille cedex

Received February 9, 2009; Revised Manuscript Received June 10, 2009

ABSTRACT: Nucleation in solution is a stochastic phenomenon and thus difficult to control. We present here an in situ investigation of the control of spatial and temporal localization on the nucleation event, using two approaches. We show how creating localized fields and fluxes and/or preventing convection lead to effective control. Thus, we will be able to explore the formation and the structure of critical nuclei and unravel the mechanisms of nucleation.

Understanding and controlling nucleation are the major focus of our work. Because nucleation is a stochastic phenomenon, spatial and temporal control of nucleation is a way to explore the formation and the structure of critical nuclei and to unravel the mechanisms of nucleation. In practice, to avoid uncontrolled nucleation due to this stochasticity, seeding techniques are often used.¹ Alternative solutions have been proposed: use of microfluidic devices,^{2,3} confined engineering surfaces,⁴ material containing nanometer-scale pores,⁵ use of finite sized systems⁶ as well as methods using an external field, either magnetic,^{7,8} electric,^{9–12} ultrasonic,¹³ or electromagnetic.^{14–19} To date, none of these approaches has succeeded in controlling both the frequency and the location of nucleation.

This communication presents a recent in situ investigation on the control of spatial and temporal localization of the nucleation event. In a previous report,²⁰ we presented an experimental setup for in situ investigation of the effect of a localized DC voltage on the nucleation and growth of proteins in the metastable zone. Our setup used a crystallization cell with two electrodes where at least one of the electrodes had a sharp tip. Because of the nanometer size of the tip, large electric fields and large field gradients were encountered near the tip for small DC voltage. This geometry also induced a high current density inside the solution close to the region of high curvature. Results on bovine pancreatic trypsin inhibitor (BPTI) and lysozyme crystallizations in the presence of an internal electric field and direct current showed that nucleation is enhanced and that crystallization is located near one electrode due to a concentration gradient between the electrodes.²⁰

Here, we have chosen BPTI at 20 mg/mL (6511 Da, pI 10.5) crystallizing at pH 4.9 in NaCl solution (1.6 M) to demonstrate the effectiveness of our experimental approach. The crystallization and visualization were performed in a thermostatted peltier cell equipped with a Nikon microscope and digital imaging capabilities, and has previously been described in detail.²¹ We made the electrode, here the anode, from tungsten (W) wires (125 μm diameter) consisting of a sharp metallic tip emerging from the end of a glass capillary; the tip is fabricated by electrolytic etching (for a more detailed description see refs 22 and 23).

Objective (1): Confine Current Lines to the Tip Apex. The idea is to coat the anode with an insulator which must be chemically inert, insoluble in water, and hydrophobic, in order to concentrate the current lines at the tip apex. In a first attempt, we coated part of the anode with Araldite (white arrows in Figure 1a). We observed, in a BPTI solution with an applied DC voltage of 0.6 V ($I = 0.5 \mu\text{A}$), that a protein rich-phase nucleates on the anode except on the coated part and that crystals grow larger near the uncoated

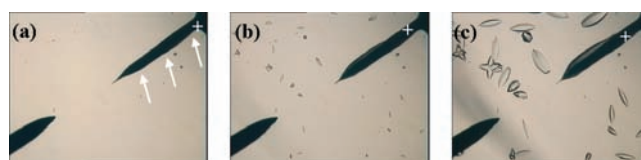


Figure 1. In-situ observations under optical microscopy, the anode being partially coated with Araldite (the white arrows indicate the coated area). In BPTI (20 mg/mL - NaCl 1.6 M) solution at 20 °C with a DC voltage $V = 0.6 \text{ V}$ and $I = 0.5 \mu\text{A}$ at time (a) 0, (b) 12, and (c) 24 h. As reference, the W-electrode wire diameter is 125 μm .

part of the anode (Figure 1b,c). The Araldite plays the role of an electrical insulator, increasing the spatial control of the electric field on the crystallization.

In a second set of experiments, we coated the anode with wax (ethylene glycol and fatty acid ester) at $T > 45 \text{ °C}$ by immersion. When the anode is withdrawn from the solution, the entire surface is coated except the tip (Figure 2a). To prove this, we performed an experiment in NaOH solution, with an applied AC voltage of 1 V. We observe bubbles only at the tip apex due to water electrolysis (Figure 2b). Similarly, in BPTI solution with an applied DC voltage of 1 V ($I = 0.66 \mu\text{A}$) nucleation of a protein rich-phase is localized at the tip alone (Figure 2c–e). These experiments clearly show that the emergence of the current lines is localized at the tip apex. Note that we previously observed with the uncoated electrode that only nucleation occurred at low voltage, whereas when the voltage was increased a protein-rich phase nucleated over the anode. This liquid–liquid phase separation (LLPS) sometimes hinders crystal nucleation.²⁴

Objective (2): Nucleate at the Tip. Convection counteracts the effect of the electric field, which tends to create a concentration gradient, by rehomogenizing the solution and suspension when nuclei and crystals are present. Therefore, Nakamura et al.^{25,26} proposed the use of a highly viscous gel medium to suppress nuclei and crystals diffusion in femtosecond laser-induced crystallization experiments. Here, to diminish convection, we operate in agarose gel (0.5% w/v)²⁷ with the uncoated electrode. The sequence presented in Figure 3 (0.6 V - 0.35 μA - nucleation time: 1 h) shows that the use of gel as crystallization medium clearly enables better control of the location of nucleation and the nucleus appears in the vicinity of the tip where the electric field is the strongest.

Objective (3): Nucleate at Will! The following experiment shows how to trigger nucleation waves. First, nucleation occurs with the wax-coated anode (Figure 4a,b) (0.8 V - 0.74 μA - nucleation time: 2 h). The voltage is lower than in the previous experiment (presented in Figure 2) in order to avoid LLPS. Second, we increase the voltage to 0.9 V (0.73 μA) and as a result a second

* To whom correspondence should be addressed. Phone: 336 6292 2866. Fax: 334 9141 8916. E-mail: veesler@cinam.univ-mrs.fr.

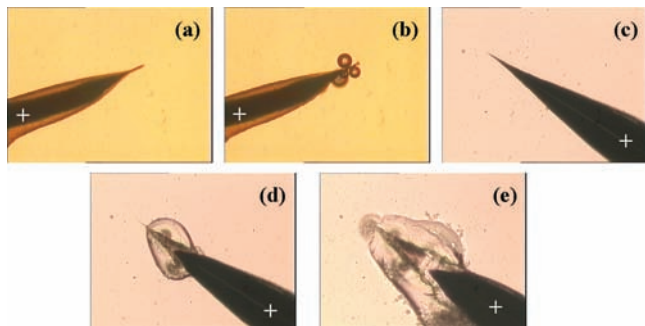


Figure 2. In-situ observations under optical microscopy, the anode being coated with wax. In NaOH 2 M solution with an AC voltage (a) $V = 0$ V and (b) $V = 1$ V; in BPTI (20 mg/mL - NaCl 1.6 M) solution at 20 °C with a DC voltage, (c), (d) and (e) $V = 1$ V and $I = 0.66 \mu\text{A}$ at time 0, 24, and 72 h. Nucleation of a dense liquid phase is observed (d) and (e). As reference, the W-electrode wire diameter is 125 μm .



Figure 3. BPTI (20 mg/mL - NaCl 1.6M) nucleation in the vicinity of the tip in 0.5% agarose gel (0.8 V - 0.74 μA), length of experiment 12 h. As reference, the W-electrode wire diameter is 125 μm .

nucleation wave occurred within 1 h (Figure 3c). Third and last, we increase the voltage again 1 V (1.40 μA) and as a result a third nucleation wave occurs within 1 h (Figure 3d). After every nucleation event, the voltage is successively increased from 0.6 to 0.9 and to 1 V in order to restore a concentration gradient high enough to allow a new nucleation wave.

These results of BPTI nucleation in the presence of an internal electric field and direct current using a wax-coated anode show

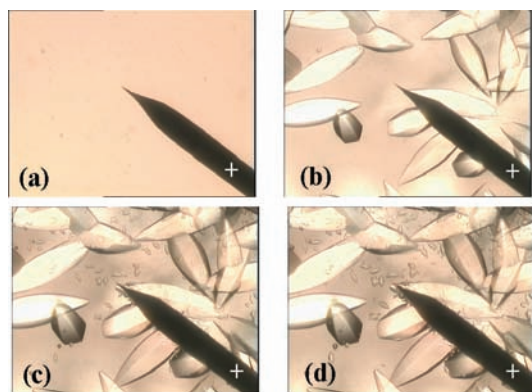


Figure 4. In-situ observations of three successive nucleation waves (characterized by three different crystal size distributions in (e)) under optical microscopy of BPTI (20 mg/mL - NaCl 1.6 M) solution at 20 °C with DC voltage, the anode being coated with wax. As reference, the W-electrode wire diameter is 125 μm .

that the current lines are confined to the tip apex, that nucleation can be triggered at will by tuning the DC voltage applied, and that the use of gel diminishes convection in solution, leading to better control of the location of nucleation. This setup clearly enables us to control the spatial and the temporal localization of the nucleation event. Thus, we will be able to explore the formation and the structure of critical nuclei and unravel the mechanisms of nucleation.

Acknowledgment. We thank Bayer A.G. (Wuppertal, Germany) for providing us with BPTI and to M. Sweetko for English revision.

References

- (1) Kubota, N.; Doki, N.; Yokota, M.; Sato, A. *Powder Technol.* **2001**, *121*, 31.
- (2) Laval, P.; Salmon, J.-B.; Joanicot, M. *J. Cryst. Growth* **2007**, *303*, 622.
- (3) Shim, J.-U.; Cristobal, G.; Link, D. R.; Thorsen, T.; Fraden, S. *Cryst. Growth Des.* **2007**, *7*, 2192.
- (4) Lee, A. Y.; Lee, I. S.; Dette, S. S.; Boerner, J.; Myerson, A. S. *J. Am. Chem. Soc.* **2005**, *127*, 14982.
- (5) Ha, J.-M.; Wolf, J. H.; Hillmyer, M. A.; D., W. M. *J. Am. Chem. Soc.* **2004**, *126*, 3382.
- (6) Grossier, R.; Veessler, S. *Cryst. Growth Des.* **2009**, *9*, 1917.
- (7) Astier, J. P.; Veessler, S.; Boistelle, R. *Acta Crystallogr.* **1998**, *D54*, 703.
- (8) Sasaki, G.; Yoshida, E.; Komatsu, H.; Nakada, T.; Miyashita, S.; Watanabe, K. *J. Cryst. Growth* **1997**, *173*, 231.
- (9) Taleb, M.; Didierjean, C.; Jelsch, C.; Mangeot, J. P.; Capelle, B.; Aubry, A. *J. Cryst. Growth* **1999**, *200*, 575.
- (10) Nanev, C. N.; Penkova, A. *J. Cryst. Growth* **2001**, *232*, 285.
- (11) Moreno, A.; Sasaki, G. *J. Cryst. Growth* **2004**, *264*, 438.
- (12) Hou, D.; Chang, H.-C. *Appl. Phys. Lett.* **2008**, *92*, 223902.
- (13) Ueno, S.; Ristic, R. I.; Higaki, K.; Sato, K. *J. Phys. Chem. B* **2003**, *107*, 4927.
- (14) Tyndall, J. *Philos. Mag.* **1896**, *37*, 384.
- (15) Tam, A.; Moe, G.; Happer, W. *Phys. Rev. Lett.* **1975**, *35*, 1630.
- (16) Garetz, B. A.; Aber, J. E.; Goddard, N. L.; Young, R. G.; Myerson, A. S. *Phys. Rev. Lett.* **1996**, *77*, 3475.
- (17) Zaccaro, J.; Matic, J.; Myerson, A. S.; Garetz, B. A. *Cryst. Growth Des.* **2001**, *1*, 5.
- (18) Okutsu, T.; Nakamura, K.; Haneda, H.; Hiratsuka, H. *Cryst. Growth Des.* **2004**, *4*, 113.
- (19) Veessler, S.; Furuta, K.; Horiuchi, H.; Hiratsuka, H.; Ferté, N.; Okutsu, T. *Cryst. Growth Des.* **2006**, *6*, 1631.
- (20) Hammadi, Z.; Astier, J. P.; Morin, R.; Veessler, S. *Cryst. Growth Des.* **2007**, *8*, 1476.
- (21) Veessler, S.; Lafferrere, L.; Garcia, E.; Hoff, C. *Org. Process Res. Dev.* **2003**, *7*, 983.
- (22) Muller E. W.; Tsong T. T. *Field Ion Microscopy: Principles and Applications*; American Elsevier Publishing Company: New York, 1969.
- (23) Hammadi, Z.; Gauch, M.; Morin, R. *J. Vac. Sci. Technol. B: Microelectron. Nanometer Struct.* **1999**, *17*, 1390.
- (24) Lafferrere, L.; Hoff, C.; Veessler, S. *Cryst. Growth Des.* **2004**, *4*, 1175.
- (25) Nakamura, K.; Sora, Y.; Yoshikawa, H. Y.; Hosokawa, Y.; Murai, R.; Adachi, H.; Mori, Y.; Sasaki, T.; Masuhara, H. *Appl. Surf. Sci.* **2007**, *253*, 6425.
- (26) Yoshikawa, H. Y.; Murai, R.; Sugiyama, S.; Sasaki, G.; Kitatani, T.; Takahashi, Y.; Adachi, H.; Matsumura, H.; Murakami, S.; Inoue, T.; Takano, K.; Mori, Y. *J. Cryst. Growth* **2009**, *311*, 956.
- (27) Budayova-Spano, M.; Bonnette, F.; Astier, J. P.; Veessler, S. *J. Cryst. Growth* **2002**, *235*, 547.

CG900150N